

PACS numbers: 42.55.Rz; 42.60.Jf; 42.60.Lh
DOI: 10.1070/QE2008v038n04ABEH013727

Formation of a beam profile at the input to a high-energy laser amplifier

M.A. Martyanov, A.K. Poteomkin, A.A. Shaykin, E.A. Khazanov

***Abstract*. A device consisting of a pin-hole line and an apodizing aperture, which provides the fill factor of the laser amplifier aperture equal to 0.8, is proposed and studied experimentally. The use of this device allowed the generation of 300-J, 1-ns pulses due to the efficient energy extraction from a six-stage neodymium phosphate glass amplifier with the final stage aperture equal to 10 cm.**

Keywords: *high-power laser amplifier, amplified radiation beam formation, efficient stored energy extraction.*

1. Introduction

To extract efficiently the energy stored in active elements (AEs) of laser amplifiers, it is necessary to use their aperture maximally. The degree of aperture filling by a radiation beam is characterised by the fill factor F. This parameter in the axially symmetric case is defined as

$$F = \frac{1}{I_{\max}\pi r_0^2}\int_0^{r_0} I(r)2\pi r\mathrm{d}r, \qquad (1)$$

where $I(r)$ is the radial intensity distribution with the maximum value $I_{\max}$ and r_0 is the AE radius. It is obvious that for an AE in which the gain is independent of transverse coordinates, a rectangular beam with sharp edges on the AE boundary is optimal. The fill factor for this beam is $F = 1$. However, the beam is distorted due to diffraction during its propagation even over distances comparable with the AE length. In addition, the method of image transfer from one amplification stage to another (the Kepler telescope with a pin hole narrowing the angle of view of the system and rejecting the spatial harmonics of small-scale self-focusing [1, 2]) does not provide the transfer of images with sharp boundaries. These two circumstances complicate the efficient use of rectangular beams in high-power laser systems. Therefore, of current interest is the problem of obtaining a beam with a high enough parameter F (above 0.8) and the transverse intensity distribution of a smoothed rectangular beam, which is similar to the intensity distribution

$$I(r) \approx I_{\max}\exp\left[-\left(\frac{r}{a}\right)^{2m}\right] \qquad (2)$$

of a super-Gaussian beam with the radius a and a high power m, but vanishing at the AE boundaries.

The inhomogeneous distribution of the gain and gain saturation in the AE lead to a change in the amplified beam profile and an increase in the fill factor, as a rule. Therefore, to obtain high output values of F, the input beam should have a somewhat lower fill factor. The problem of obtaining the maximum value F at the amplifier output requires the consideration of all the factors mentioned above, which are not always well defined; therefore, it is more reasonable to solve the problem of increasing the fill factor F for radiation incident on the amplifier.

If a repetitively pulsed laser is used as a master oscillator, the propagation direction and wave-front curvature of radiation can change due to a high heat release in the AE during its operation. A system for radiation coupling should reduce such variations. This system should also provide the smoothing of fluctuations of the transverse intensity distribution, i.e. perform the spatial filtration of incident radiation. It is also necessary to specify the direction along which the amplifier should be adjusted and to provide the required accuracy of radiation propagation along this direction with the help of auxiliary mirrors. In other words, not only the intensity distribution (2) but also the beam phase at the input to a high-power laser amplifier should weakly depend on field fluctuations at the input to the radiation coupling system.

In this paper, we describe an input spatial filter (ISF) which satisfies to a certain degree all the requirements mentioned above. This ISF was used to couple radiation from a low-power Nd : YLF laser with a pulse repetition rate of 1 Hz into a six-stage neodymium phosphate glass amplifier (the output pulse energy was up to 300 J) [3].

2. Principles of the beam profile formation

The key element of an ISF is apodization unit (*8*), (*9*), (*10*) (Fig. 1) consisting of soft aperture (*8*), rigid aperture (*9*), and polariser (*10*). Soft aperture (*8*) is a crystal quartz lens in optical contact with a fused silica lens [4]. Such a doublet modulates polarisation of the initially linearly polarised radiation, by forming ring zones. Output polariser (*10*) transforms the polarisation modulation to the

M.A. Martyanov, A.K. Poteomkin, A.A. Shaykin, E.A. Khazanov
Institute of Applied Physics, Russian Academy of Sciences, ul. Ul'yanova 46, 603950 Nizhnii Novgorod, Russia;
e-mail: khazanov@appl.sci-nnov.ru

Received 28 August 2007; revision received 9 October 2007
Kvantovaya Elektronika **38** (4) 354 – 358 (2008)
Translated by M.N. Sapozhnikov

intensity modulation. If the first dark ring of the soft aperture is made coincident with rigid aperture (*9*), the entire system will have the intensity transmission coefficient

$$t_a(r) = \begin{cases} \sin^2\left[\dfrac{\pi\delta}{2}\left(1-\dfrac{r^2}{r_0^2}\right)\right], & r < r_0, \\ 0, & r \geqslant r_0, \end{cases} \quad (3)$$

where parameters δ and r_0 are determined by the geometrical characteristics of the soft aperture. The radius r_0 will further determine the beam aperture. If $\delta = 1$, the transmission coefficient is $t_a(r) = \cos^2(\frac{1}{2}\pi r^2/r_0^2)$ and such a soft aperture is sometimes called a cosine-aperture.

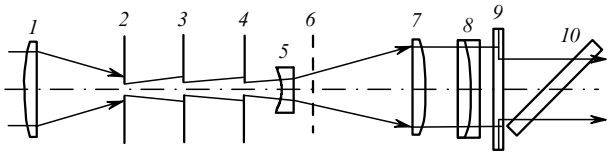

Figure 1. Scheme of the ISP: (*1*) input focusing lens; (*2*, *3*, *4*) pin-hole line; (*5*, *7*) telescope; (*6*) image plane; (*8*, *9*, *10*) apodization unit [(*8*) soft cosine-aperture, (*9*) rigid aperture, (*10*) polariser].

The main parameters of a soft aperture are the integrated (over the cross section) transmission coefficient T_a and fill factor F. The product T_aF can characterise the quality of the soft aperture and ISF as a whole. When a plane wave is incident on the pin hole with transmission (3), a beam is formed with intensity proportional to $t_a(r)$. The fill factor for such a beam is $F = 0.5$ and $T_a \to 0$. If $\delta \neq 1$, a beam with a dip at the centre of the intensity distribution is formed, for which F depends on δ and achieves the maximum $F = 0.55$ for $\delta = 1.17$, but $T_a \to 0$ in this case. If the soft aperture with transmission (3) is illuminated by a beam with the Gaussian intensity profile of radius $a = 0.82r_0$ at which 50 % of energy is transmitted by the aperture, the fill factor of the aperture is $F = 0.34$ and $T_aF = 0.167$. If it is required that the fill factor should be at least 0.45, the transmission of the aperture will be 0.16 for $T_aF = 0.074$. For $\delta \neq 1$, it is also difficult to obtain high values of T_aF.

Thus, to obtain $F = 0.5 - 0.6$ at the soft aperture output for the acceptable integrated transmission T_a, it is necessary to have a minimum at the centre of the intensity distribution of the incident beam. Such a field structure can be obtained in the near-field diffraction zone for a pin hole. Let us find at which distances from a pin hole the field distribution with the required dip on the axis can be obtained.

In the case of the radial symmetry, the propagation of the field in the paraxial approximation is described by the Kirchhoff–Fresnel integral [5]

$$V(r,z) = \frac{ik}{z}\exp(ikz)\exp\left(\frac{ikr^2}{2z}\right)\int_0^R \exp\left(\frac{ikr_1^2}{2z}\right) \times J_0\left(\frac{krr_1}{z}\right)V_0(r_1)r_1\,dr_1, \quad (4)$$

where $k = 2\pi/\lambda$; λ is the wavelength; $V_0(r_1)$ is the field in the cross section $z = 0$; and J_0 is the zero-order Bessel function. Let us assume that a pin hole of radius R located in the cross section $z = 0$ is illuminated by a Gaussian beam whose field in the pin-hole plane has the form

$$V_0(r_1) = \exp\left(-\frac{r_1^2}{2a^2} - \frac{ikr_1^2}{2f}\right)$$

in the general case. Here, a determines the beam width and f determines its wave-front curvature in the pin-hole plane. It is assumed that the beam is focused for $f > 0$, i.e. the common rule for lens signs is used. The radiation intensity on the axis ($r = 0$) at a distance of z from the pin hole is determined by the relation

$$I(z) = |V(r=0,z)|^2 = \left[\exp\left(-\frac{R^2}{a^2}\right) + 1 - 2\exp\left(-\frac{R^2}{2a^2}\right)\cos\left(\frac{kR^2}{2z} - \frac{kR^2}{2f}\right)\right] \times \left[\left(1-\frac{z}{f}\right)^2 + \left(\frac{z}{ka^2}\right)^2\right]^{-1}. \quad (5)$$

Figue 2 presents the dependences of the intensity I on the beam axis on the longitudinal coordinate z for different values of a/R and $f \to \infty$. If a plane wave is incident on the pin hole, i.e. $a, f \to \infty$, the intensity on the axis is described by the oscillating function

$$I(z) \propto 2\left(1 - \cos\frac{kR^2}{2z}\right)$$

with the last maximum located at a distance of $z^* = R^2/\lambda$. As the ratio a/R is decreased, the maxima decrease and shift to the left. It follows from these dependences that characteristic distances at which the field distribution has the required configuration lie within the range

$$0.5 < \frac{\lambda z}{R^2} < 1. \quad (6)$$

The ISF scheme presented in Fig. 1 can be used to obtain a beam with a dip in the intensity distribution in the plane of cosine-aperture (*8*). Lens (*1*) focuses a linearly polarised beam on pin hole (*2*) separated from lens (*1*) by a distance that is not equal to the focal distance of the lens in the general case. Then, the beam diffracts successively from pin holes (*2*), (*3*), and (*4*) (the number of pin holes can be larger in the general case), is expanded in telescope (*5*), (*7*) and is incident on soft aperture (*8*), rigid aperture (*9*), and

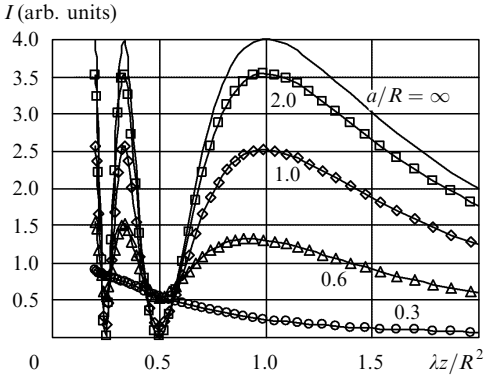

Figure 2. Dependences of the radiation intensity I on the beam axis on $\lambda z/R^2$ calculated by expression (5) for $f \to \infty$ and different ratios a/R.

polariser (*10*). Distances between elements (*4*), (*5*), (*7*), (*8*) are selected in such a way that the image of plane (*6*) with a dip on the axis in the intensity distribution is transferred to the plane of soft aperture (*8*) with magnification provided by telescope (*5*), (*7*). The integrated transmission coefficient $T = T_d T_a$ of the ISF is determined by the transmission coefficient T_d of pin-hole line (*2*), (*3*), (*4*) and the transmission coefficient T_a of apodization unit (*8*), (*9*), (*10*).

The pin-hole line was optimised as the main selecting element by considering three variants of its construction: equidistant, quasi-equidistant, and non-equidistant.

The equidistant pin-hole line consists of pin holes of the same diameter spaced equidistantly in succession. This line is characterised by the Fresnel number $N = R^2/(\lambda L)$ (where R is the radius of pin holes and L is the distance between them), while the field distribution $\Psi(\boldsymbol{r})$ in its modes (in the radially symmetric case, these are Fox–Li modes [6]) is determined by the integral equation

$$\Lambda\Psi(\boldsymbol{r}_2) = 2\pi i N \int_S \exp\left[\frac{2\pi i N(\boldsymbol{r}_2 - \boldsymbol{r}_1)^2}{2}\right]\Psi(\boldsymbol{r}_1)\mathrm{d}^2\boldsymbol{r}_1, \quad (7)$$

where $\boldsymbol{r}_{1,2}$ are dimensionless radius vectors. The mode structure and eigenvalues Λ, which determine, in particular, the decay of modes during their propagation, are specified by the only number parameter N.

The quasi-equidistant pin-hole line with a constant magnification and a constant reciprocal Fresnel number consists of pin holes with gradually increasing diameter, the ratio of radii of pin holes at each stage $M = R_{n+1}/R_n$ (where n is the stage number) and the reciprocal Fresnel number $N = R_{n+1}R_n/(\lambda L_n)$ being constant. The integral equation for this line has the form

$$\Lambda\Psi(\boldsymbol{r}_2) = 2\pi i \frac{N}{M}\int_S \exp\left[2\pi i \frac{N}{M}\frac{(M\boldsymbol{r}_2 - \boldsymbol{r}_1)^2}{2}\right]\Psi(\boldsymbol{r}_1)\mathrm{d}^2\boldsymbol{r}_1. \quad (8)$$

Such a line is not equidistant in the general case; however, it also has modes and eigenvalues, which are already determined by two parameters M and N.

The non-equidistant pin-hole line has even greater number of degrees of freedom (radii and distances between pin holes), it is characterised by many quantitative parameters, unlike the two parameters (the Fresnel number and ratio M), as in the quasi-equidistant case, and therefore is inconvenient for calculations. However, these degrees of freedom can be used to improve the parameters of the ISF at final stages of calculations, when the main ISF parameters have been determined more or less by using simpler considerations.

3. Parameters of an input spatial filter

We calculated and optimised an ISP used for matching a beam from a repetitively pulsed laser with a neodymium phosphate glass amplifier with the maximum pulse energy of 300 J [3] by assuming that the radiation wavelength was 1054 nm, the diameter of a beam incident on the ISP was 5 mm and the transverse intensity distribution in the beam was close to rectangular. The focal distance of lens (*1*) (see Fig. 1) was set equal to 3 m and the focal distances of telescope lenses (*5*) and (*7*) were 25.4 and 172 mm, respectively. In addition, we assumed that a beam with the intensity distribution having a dip at its centre should be incident on the soft aperture in order to achieve the fill factor $F = 0.5 - 0.6$ at the integrated transmission coefficient of the ISP $T = 0.1 - 0.05$.

The problem of maximisation of the fill factor at the ISP output was solved at some additional restrictions. The ISP length (measured from the first pin hole) should not exceed 3 m (for the ISP to be mounted on a standard optical table), while the energy density on lens (*5*) should be smaller than 3 J cm^{-2}, i.e. lower than the breakdown level for telescope lenses in the case of nanosecond pulses. The radiation intensity on the edges of all pin holes should not be too high to avoid the closing of pin holes by a plasma appearing on their surface [7, 8]. The transmission coefficient of a pin-hole line was restricted from below ($T_d \gtrsim 0.4 - 0.5$) to avoid the degeneracy of the line to an interval in free space (the excessive increase in the pin-hole diameter or a decrease in their separation) during the operation of the calculation algorithm.

The field was calculated before plane (*6*) (Fig. 1) by using successively the Kirchhoff–Fresnel integral (4), and then – by the method of geometrical optics. By performing numerical calculations based on the data presented above, we constructed the ISP with the following parameters: the distance from lens (*1*) to pin hole (*2*) was 2680 mm, the diameters of pin holes (*2*), (*3*), and (*4*) were 1.2, 1.6, and 2.2 mm, respectively, for distances between them 570 and 1155 mm, the distance from pin hole (*4*) to lens (*5*) was 1050 mm, and the diameter of the soft aperture was 9 mm.

The calculated and experimental near- and far-field output intensity distributions of the ISF are presented in Figs 3 and 4. The near-field intensity distribution (Fig. 3) is well approximated by super-Gaussian function (2) with the parameter $m = 3.9$ and radius $a = 3.7$ mm. The output IFS beam had the aperture fill factor $F = 0.6$ and diffraction quality (Fig. 4). In this case, the transmission coefficients of the pin-hole line, apodization unit, and entire ISF were 0.43, 0.19, and 0.08, respectively.

An important characteristic of the ISF is its selecting properties – the degree of suppression of the incident field distortions. The most important are, in our opinion, phase distortions of the field, namely, linear and quadratic (in coordinates) additions to the phase. The former are responsible for a change in the propagation angle of the incident field, the latter – for its geometric-optics divergence. It follows from the theory of moments [9] that the centre of mass of a beam in a homogeneous linear medium propagates along a straight line. We will call the slope of this straight line with respect to the ISF axis the propagation angle of the field. For small angles, the dependence of the field propagation angle β behind the ISF on the propagation angle α before the ISF can be approximated by a straight line. The slope of this straight line $\gamma_1 = (\mathrm{d}\beta/\mathrm{d}\alpha)_{\alpha=0}$ characterises the suppression of deviation from the propagation direction of input radiation by the ISF.

Similarly, we can introduce the criterion for suppression of the geometrical component of the radiation divergence $\gamma_2 = (\mathrm{d}R_{in}/\mathrm{d}R_{out})_{R_{in}\to\infty} \to 0$, where R_{in} and R_{out} are the geometrical components of the divergence of radiation incident on the ISF and emerging from it. One of the initial variants of the ISF [10] had good selecting properties ($\gamma_1 = 0.2$ and $\gamma_2 = 0.02$), the transmission of the pin-hole line in the regime without screening the laser beam by plasma $T_d = 0.54$, the integrated transmission $T = 0.09$, and

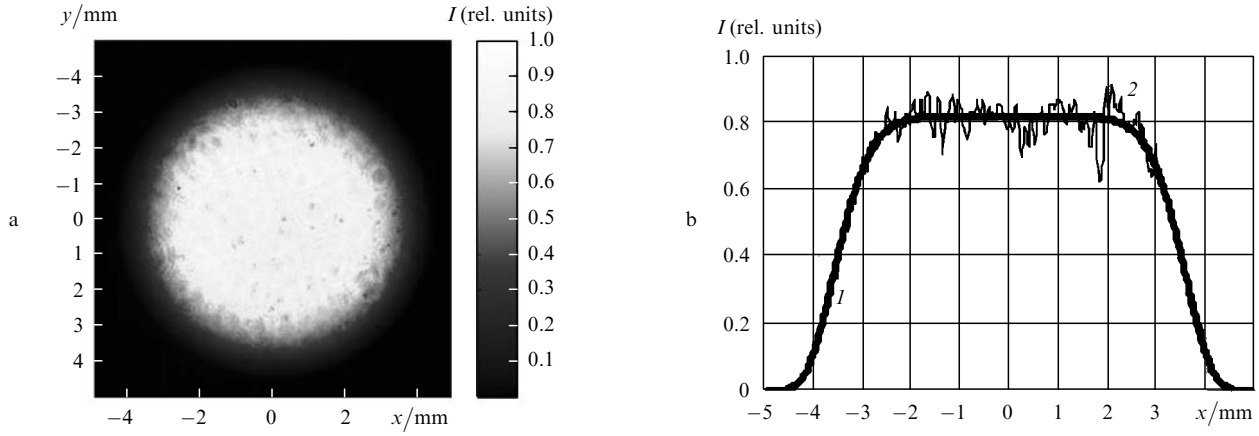

Figure 3. Near-field intensity distribution map for the ISP output beam (a) and the intensity distributions in the central section of this zone approximated by expression (2) for $m = 3.9$ (*1*) and experimentally measured (*2*) (b).

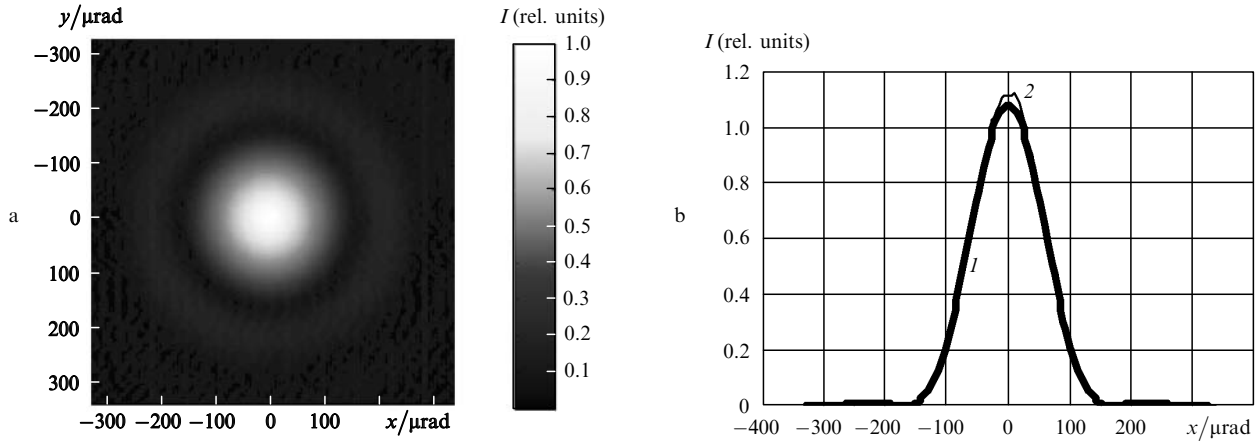

Figure 4. Far-field intensity distribution map for the ISP output beam (in the focal plane of an aberration-free objective with a focal distance of 1.2 m) (a) and the Fourier limit calculated from the near-field intensity distribution in Fig. 3 (*1*) and the experimental intensity distribution at the central section of the far-field zone (*2*) (b).

the AE aperture fill factor after apodization $F = 0.4$. The ISF considered in this paper has $\gamma_1 = 0.15$, $\gamma_2 = 0.014$, $T_d = 0.53$, $T = 0.08$, and $F = 0.6$. Thus, we have managed to increase considerably the AE fill factor at the ISF output compared to [10] and have improved the selecting properties of the pin-hole line at virtually the same transmission.

The symmetry of the radial intensity distribution at the ISF output strongly affects the adjustment accuracy. The output ISF radiation obtained in experiments (Fig. 3) allows one to adjust the laser beam in the amplifier with an error of ~ 10 μrad. This amounts to 1/12 of the diffraction divergence of radiation propagated through the ISF (Fig. 4).

Figure 5 shows the near- and far-field intensity distributions of the output beam (after amplification up to 300 J in a 1-ns pulse) obtained on the setup [3] in which the ISF described above was used. The transverse near-field radiation intensity distribution (Fig. 5a) before the last expanding telescope has a diameter of 93 mm and is sufficiently uniform: $F = 0.87$. The intensity distribution in the focal plane of a diagnostic objective with the focal distance 3 m (far-field zone., Fig. 5b) is close to the diffraction limit.

4. Conclusions

The theoretical and experimental study of the system for formation of the transverse intensity profile of the output beam described in the paper has shown that this system can be efficiently used for matching a repetitively pulsed Nd : YLF laser and a high-power (300 J in a 1-ns pulse) neodymium phosphate glass amplifier. The use of the ISP considerably simplified the alignment of the Nd : YLF laser beam in the amplifier and improved the angular accuracy (to 1/10 of the diffraction limit) of coupling the laser beam into the amplifier. The fill factor F of the amplifier aperture at the output of the setup achieved 0.87, which resulted in almost triple increase in the output pulse energy by preserving the output AE aperture. The selecting properties of the ISP allowed us to adjust the laser once per day, and then 10–15 shots were performed for a day already without adjustment. The second harmonic of this laser was used to pump the output stage of a superbroadband parametric amplifier, which allowed us to achieve the output peak power of the femtosecond laser complex up to ~ 0.56 PW [3].

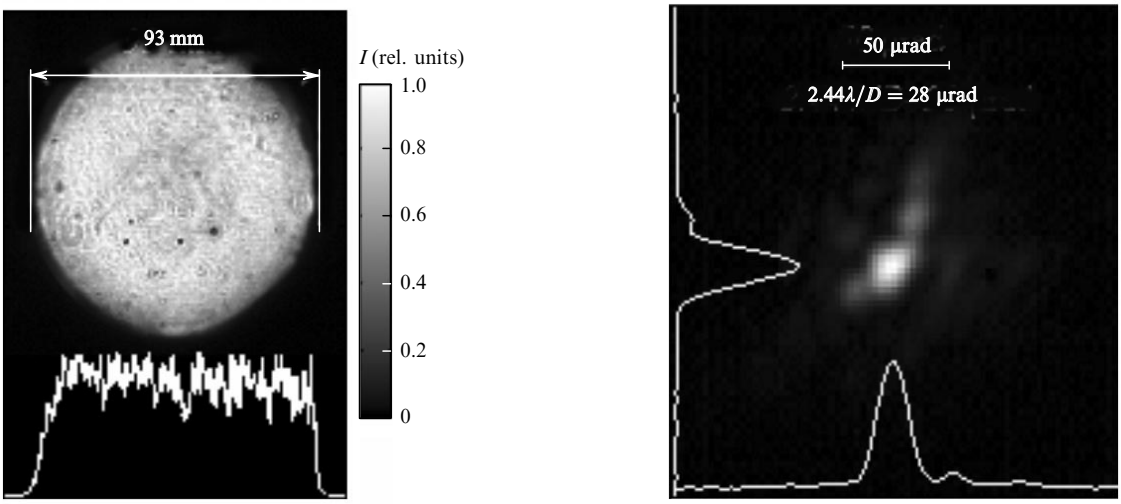

Figure 5. Intensity distributions in the near-field (a) and far-field (in the focal plane of an aberration-free objective with a focal distance of 3 m) (b) diffraction zones for the output beam (after amplification up to 300 J in a 1-ns pulse) obtained on the laser setup [3]; $D = 2R$.

References

1. Kuz'mina N.V., Rozanov N.N., Smirnov V.A. *Opt. Spektrosk.*, **51**, 509 (1981).
2. Bunkenderg J. *IEEE J. Quantum Electron.*, **17** (9), 1620 (1981).
3. Lozhkarev V.V., Freidman G.I., Ginzburg V.N., Katin E.V., Khazanov E.A., Kirsanov A.V., Luchinin G.A., Mal'shakov A.N., Martyanov M.A., Palashov O.V., Poteomkin A.K., Sergeev A.M., Shaykin A.A., Yakovlev I.V. *Laser Phys. Lett.*, **4** (6), 421 (2007).
4. Papernyi S.B., Serebryakov V.A., Yashin V.E. *Kvantovaya Elektron.*, **5**, 2059 (1978) [*Sov. J. Quantum Electron.*, **8**, 1165 (1978)].
5. Born M., Wolf E. *Principles of Optics* (Oxford: Pergamon Press, 1969; Moscow: Nauka, 1973).
6. Fox A.G., Li T. *Bell Systems Technol. J.*, **40** (2), 453 (1961).
7. Bikmatov R.G., Boley C.D., Burdonski I.N., Chernyak V.M., Fedorov A.V., Goltsov A.Y., Kondrashov V.N., Koptyaev S.N., Kovalsky N.G., Kuznetsov V.N., Milam D., Murray J., Pergament M.I., Petryakov V.M., Smirnov R.V., Sokolov V.I., Zhuzhukalo E.V. *Proc. SPIE Int. Soc. Opt. Eng.*, **3492**, 510 (1998).
8. Speck D.R. *IEEE J. Quantum Electron.*, **17** (9), 1599 (1981).
9. Vlasov S.N., Petrishchev V.A., Talanov V.I. *Izv. Vyssh. Uchebn. Zaved., Ser. Radiofiz.*, **14**, 1353 (1971).
10. Potemkin A.K., Katin E.V., Kirsanov A.V., Luchinin G.A., Mal'shakov A.N., Mart'yanov M.A., Matveev A.Z., Palashov O.V., Khazanov E.A., Shaikin A.A. *Kvantovaya Elektron.*, **35**, 302 (2005) [*Quantum Electron.*, **35**, 302 (2005)].